J. KSIAM Vol.21, No.4, 245–275, 2017 http://dx.doi.org/10.12941/jksiam.2017.21.245

DUFOUR AND HEAT SOURCE EFFECTS ON RADIATIVE MHD SLIP FLOW OF A VISCOUS FLUID IN A PARALLEL POROUS PLATE CHANNEL IN PRESENCE OF CHEMICAL REACTION

M. VENKATESWARLU[1†], R. VASU BABU[2], AND S.K. MOHIDDIN SHAW[3]

[1] DEPARTMENT OF MATHEMATICS, V. R. SIDDHARTHA ENGINEERING COLLEGE, KANURU, VIJAYAWADA, KRISHNA (DIST), ANDHRA PRADESH, INDIA
E-mail address: mvsr2010@gmail.com

[2] DEPARTMENT OF MATHEMATICS, SHRI VISHNU ENGINEERING COLLEGE, FOR WOMEN, BHIMAVARAM, WEST GODAVARI (DIST), ANDHRA PRADESH, INDIA
E-mail address: vasukgr@gmail.com

[3] DEPARTMENT OF MATHEMATICS, NARASARAOPTA ENGINEERING COLLEGE, NARASARAOPETA, GUNTUR (DIST), ANDHRA PRADESH, INDIA
E-mail address: mohiddin_shaw26@yahoo.co.in

ABSTRACT. The present investigation deals, Dufour and heat source effects on radiative MHD slip flow of a viscous fluid in a parallel porous plate channel in presence of chemical reaction. The non-linear coupled partial differential equations are solved by using two term perturbation technique subject to physically appropriate boundary conditions. The numerical values of the fluid velocity, temperature and concentration are displayed graphically whereas those of shear stress, rate of heat transfer and rate of mass transfer at the plate are presented in tabular form for various values of pertinent flow parameters. By increasing the slip parameter at the cold wall the velocity increases whereas the effect is totally reversed in the case of shear stress at the cold wall. It is observed that the effect of Dufour and heat source parameters decreases the velocity and temperature profiles.

1. INTRODUCTION

At the macroscopic level it is well accepted that the boundary condition for a viscous fluid at a solid wall is one of "no-slip", i.e., the fluid velocity matches the velocity of the solid boundary. While the no-slip boundary condition has been proven experimentally to be accurate for a number of macroscopic flows, it remains on assumption that is not based on physical principles. In fact, nearly two hundred years ago Navier [1] proposed a general boundary condition that incorporates the possibility of fluid slip at a solid boundary. Navier's proposed

Received by the editors May 31 2017; Accepted December 9 2017; Published online December 18 2017.
2000 *Mathematics Subject Classification.* 76SXX, 76D10, 80A32, 80A20, 92E20.
Key words and phrases. Dufour effect, Heat source, Parallel plate channel, MHD fluid, Chemical reaction, Porous medium.
† Corresponding author.

condition assumes that the velocity v_x at a solid surface is proportional to the shear stress at the surface

$$v_x = \gamma \frac{dv_x}{dy}$$

where γ is the slip strength or slip coefficient. If $\gamma = 0$ then the general assumed no-slip boundary condition is obtained. If γ is finite, fluid slip occurs at the wall but its effect depends upon the length scale of the flow. The above relation states that the velocity of the fluid at the plates is linearly proportional to the shear stress at the plate.

NOMENCLATURE

h	channel width	A	positive real constant
a^*	mean absorption coefficient	B_0	uniform magnetic field
C	species concentration	C_f	skin-friction coefficient
c_p	specific heat at constant pressure	c_s	concentration susceptibility
Du	Dufour number	q_w	heat flux
Da	Darcy parameter	D_m	chemical molecular diffusivity
C_1	species concentration at the heated wall	C_o	species concentration at the cold wall
Gm	Solutal Grashof number	Gr	thermal Grashof number
g	acceleration due to gravity	H	non-dimensional heat source term
j_w	mass flux	K	dimensional porous medium
K_r^*	dimensional chemical reaction parameter	Kr	non-dimensional chemical reaction parameter
K_T	thermal conductivity of the fluid	M	magnetic parameter
N	radiation parameter	Nu	Nusselt number
n	frequency of oscillation	Pr	Prandtl number
Q	non-dimensional absorption of radiation parameter	Q_o	dimensional heat source parameter
Q_1	dimensional absorption of radiation parameter	q_r	radiating flux vector
Sh	Sherwood number	Sc	Schmidt number
T_1	fluid temperature at heated wall	T	fluid temperature
t	dimensional time	T_o	fluid temperature at cold wall
v	fluid velocity in y- direction	u	fluid velocity in x- direction
		V_o	scale of suction velocity

Greek symbols

β_c	coefficient of concentration expansion	β_T	coefficient of thermal expansion
ν	kinematic coefficient of viscosity	ω	A scaled frequency
ϕ_1	dimensional cold wall slip parameter	ϕ_2	dimensional heated wall slip parameter
ρ	fluid density	σ_e	electrical conductivity
τ	non dimensional time	τ_w	shear stress
ξ	A scaled coordinate	η	A scaled coordinate
ψ	A scaled velocity	θ	A scaled temperature
ϕ	A scaled concentration	γ	non-dimensional cold wall slip parameter
σ^*	Stefan-Boltzmann constant		
σ	non-dimensional heated wall slip parameter		

Due to numerous engineering applications many authors have studied and reported results on slip flows over various geometries. The effect of slip flow on the hydrodynamic boundary layer over a flat plate has been investigated by Martin and Boyd [2] who used the Maxwell slip condition. The slip flow model was extended by Anderson [3] to a stretching surface and by Fang and Lee [4] to a moving flat plate. Yu and Ameel [5] investigated on slip-flow heat transfer in rectangular micro-channels. Soltani and Yilmazer [6] discussed on slip velocity and slip layer thickness in flow of concentrated suspensions. Vedantam and Parthasarathy [7] extended the work of Ref. [2] with three different models of slip boundary conditions. Martin and Boyd [8] further studied the momentum and heat transfer in a laminar boundary layer flow over an isothermal flat plate under slip boundary conditions. This analysis takes into account, for the first time, of the variation of the stream function and temperature field with the slip parameter. Venkateswarlu and Padma [9] presented the unsteady MHD free convective heat and mass transfer in a boundary layer flow past a vertical permeable plate with thermal radiation and chemical reaction using slip condition. Watanebe et al. [10] investigated on slip of Newtonian fluids at solid boundary. Ruckenstein and Rajora [11] investigated on the no-slip boundary conditions of hydrodynamics. Cao and Baker [12] studied the mixed convective flow and heat transfer from a vertical isothermal plate with velocity-slip and temperature-jump boundary conditions, and gave local non similar solutions to the boundary layer equations. Aziz [13] considered a boundary layer slip flow over a flat plate under constant heat flux condition by using local similarity approach. Venkateswarlu et al. [14] studied the slip velocity distribution on MHD oscillatory heat and mass transfer flow of a viscous fluid in a parallel plate channel. Bhattacharyya et al. [15] analyzed and numerically solved magnetohydro-dynamic (MHD) boundary layer equations of slip flow and heat transfer over an isothermal flat plate by using shooting method. Martin and Boyd [16] studied Falkner–Skan flow over a wedge with slip boundary conditions. Rahman and Eltayeb [17] have studied a convective slip flow over a wedge with thermal jump taking into account the variability of viscosity and thermal conductivity. The boundary layer equations are transformed into ordinary ones and are solved

numerically. Coutte flow with slip and jump boundary conditions under steady state conditions and only for gases have been investigated by Marques et al. [18]. Turkyilmazoglu [19] gives multiple analytic solutions of heat and mass transfer of MHD slip flow over a stretching surface for two types of viscoelastic fluids by using the slip model of Anderson [3].

The combined effects of heat and mass transfer with chemical reaction are of great importance to scientists and engineers because of its almost universal occurrence in many branches of science and engineering and hence received a considerable amount of attention in recent years. The study of chemical reaction with heat transfer in porous medium has important engineering applications e.g. oxidation of solid materials, tubular reactors and synthesis of ceramic materials. There are two types of reactions such as (i) homogeneous reaction and (ii) heterogeneous reaction. A homogeneous reaction occurs uniformly throughout the given phase, whereas heterogeneous reaction takes place in a restricted region or within the boundary of a phase. The effect of a chemical reaction depends on whether the reaction is homogeneous or heterogeneous. A chemical reaction is said to be first-order, if the rate of reaction is directly proportional to concentration itself. In many industrial process involving flow and mass transfer over a moving surface, the diffusing species can be generated or absorbed due to some kind of chemical reaction with the ambient fluid which can greatly affect the flow and hence the properties and quality of the final product. These processes take place in several industrial applications, such as the polymer production and the manufacturing of ceramics or glassware. Thus we are particularly interested in cases in which diffusion of the species and chemical reaction occurs at roughly the same speed in analyzing the mass transfer phenomenon. Das et al. [20] have studied the effect of homogeneous first-order chemical reaction on the flow past an impulsively started infinite vertical plate with uniform heat flux and mass transfer. Manjula et al. [21] presented the influence of thermal radiation and chemical reaction on MHD flow, heat and mass transfer over a stretching surface. Muthucumarswamy and Ganesan [22] investigated the diffusion and first-order chemical reaction on impulsively started infinite vertical plate with variable temperature. Prasad et al. [23] studied the influence of reaction rate on the transfer of chemically reactive species in the laminar, non-Newtonian fluid immersed in porous medium over a stretching sheet. Venkateswarlu et al. [24-25] have studied the diffusion-thermo effects on MHD flow past an infinite vertical porous plate in the presence of radiation and chemical reaction. The problem of chemically reactive species of non-Newtonian fluid in a porous medium over a stretching sheet was investigated by Akyildiz et al. [26]. Ghaly and Seddeek [27] have investigated the effect of chemical reaction, heat and mass transfer on laminar flow among a semi-infinite horizontal plate with temperature dependent viscosity.

The heat transfer enhancement is one of the most important technical aims for engineering systems due to its wide applications in electronics, heat exchangers technology, cooling systems, development of metal waste from spent nuclear fuel, fire and combustion modelling, next-generation solar film collectors, applications in the field of nuclear energy and various thermal systems.Sparrow and Cess [28] were one of the initial investigators to consider temperature dependent heat absorption on steady stagnation point flow and heat transfer. Venkateswarlu et al. [29-31] investigated on Thermal diffusion and radiation effects on unsteady MHD free

convection heat and mass transfer flow past a vertical porous plate. Ishak [32] worked mixed convection boundary layer flow over a horizontal plate with thermal radiation.

The objective of the present study is to investigate the Dufour and heat source effects on radiative MHD slip flow of a viscous fluid in a parallel porous plate channel in presence of chemical reaction. Therefore, in the present work, the physical problem as described in Venkateswarlu et al. [33] is considered. We should in prior emphasize that our intention is not to reproduce the results of Venkateswarlu et al. [33]. In fact, the model that we consider differs considerably from that of Venkateswarlu et al. [33] in that we use a better approach in the formulation; introduce a Dufour effect and radiation of absorption parameter. The conservation equations are non-dimensionalized and solved analytically subject to appropriate boundary conditions. The following strategy is pursued in the rest of the paper. Section two presents the formation of the problem. The analytical solutions are presented in section three. Results are discussed in section four and finally section five provides a conclusion of the paper.

2. FORMATION OF THE PROBLEM

We consider unsteady two-dimensional non-linear MHD convective slip flow of an incompressible, viscous and electrically conducting fluid past a channel with non-uniform wall temperature bounded by two parallel plates separated by a distance h. The channel is assumed to be filled with a saturated porous medium. A uniform transverse magnetic field of magnitude B_o is applied perpendicular to the plates in the presence of thermal and concentration buoyancy effects. The above plate is heated at a constant temperature. It is assumed that there exist a homogeneous first order chemical reaction with constant rate K_r^* between the diffusing species and the fluid. Initially i.e. at time $t \leq 0$, both the fluid and plate are at rest and at uniform temperature T_o. Also species concentration within the fluid is maintained at uniform concentration C_o. The transversely applied magnetic field and magnetic Reynolds number are assumed to be very small so that the induced magnetic field and the Hall effects are negligible. Geometry of the problem is presented in Fig. 1. We choose a Cartesian coordinate system $(x,\, y)$ where x- lies along the centre of the channel, y- is the distance measured in the normal section such that $y = h$ is the channel's width as shown in the figure below. The governing equations for this investigation are based on the balances of mass, linear momentum, energy and concentration species. Taking into consideration these assumptions, the equations that describe the physical situation can be written in Cartesian frame of references, as follows:

Continuity equation:

$$\frac{\partial v}{\partial y} = 0 \tag{2.1}$$

Momentum equation:

$$\frac{\partial u}{\partial t} + v\frac{\partial u}{\partial y} = -\frac{1}{\rho}\frac{dp}{dx} + \nu\frac{\partial^2 u}{\partial y^2} - \frac{\sigma_e B_0^2}{\rho}u - \frac{\nu}{K}u + g\beta_T\,(T - T_0) + \, g\beta_C\,(C - C_0) \tag{2.2}$$

Energy equation:

$$\frac{\partial T}{\partial t}+v\frac{\partial T}{\partial y}=\frac{K_T}{\rho c_p}\frac{\partial^2 T}{\partial y^2}-\frac{Q_o}{\rho c_p}\left(T-T_0\right)+\frac{Q_1}{\rho c_p}\left(C-C_0\right)+\frac{D_m K_T}{c_s c_p}\frac{\partial^2 C}{\partial y^2}-\frac{1}{\rho c_p}\frac{\partial q_r}{\partial y} \quad (2.3)$$

Diffusion equation;

$$\frac{\partial C}{\partial t}+v\frac{\partial C}{\partial y}=D_m\frac{\partial^2 C}{\partial y^2}-K_r^*\left(C-C_0\right) \quad (2.4)$$

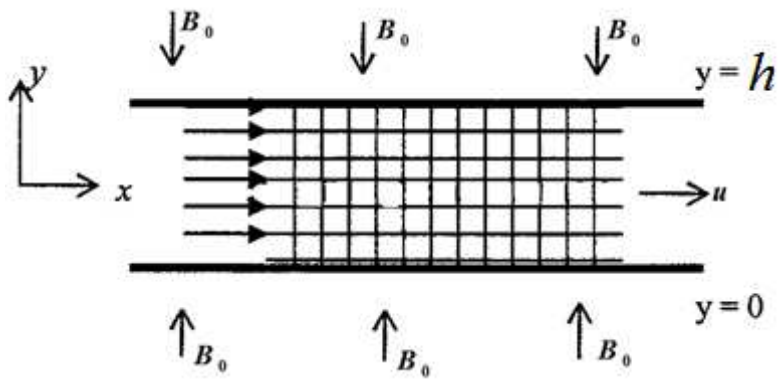

FIGURE 1. Physical model of the problem

where u- fluid velocity in x- direction, v- fluid velocity along y- direction, p- fluid pressure, g- acceleration due to gravity, ρ- fluid density, β_T- coefficient of thermal expansion, β_C- coefficient of concentration volume expansion, t- time, K- permeability of porous medium, B_o- magnetic induction, T- fluid temperature, T_o- temperature at the cold wall, K_T- thermal conductivity of the fluid, Q_o- dimensional heat source parameter, Q_1- coefficient of proportionality of the absorption of the radiation, c_s- concentration susceptibility, q_r- radiative heat flux, C- species concentration in the fluid, C_o- concentration at the cold wall, σ_e- fluid electrical conductivity, c_p- specific heat at constant pressure, D_m- chemical molecular diffusivity, ν- kinematic viscosity of the fluid and K_r^*- non-dimensional chemical reaction parameter respectively.

Under the assumption, the appropriate boundary conditions for velocity involving slip flow, temperature and concentration fields are defined as

$$\left.\begin{array}{l} u=\phi_1 u', T=T_0, C=C_0 \quad \text{at} \quad y=0 \\ u=\phi_2 u', T=T_1+\varepsilon\left(T_1-T_o\right)\exp\left(int\right), \\ C=C_1+\varepsilon\left(C_1-C_o\right)\exp\left(int\right) \quad \text{at} \quad y=h \end{array}\right\} \quad (2.5)$$

where T_1- fluid temperature at the heated plate, C_1- species concentration at the heated plate, ϕ_1- cold wall dimensional slip parameter, ϕ_2- heated wall dimensional slip parameter, n- frequency of oscillation and $\varepsilon \ll 1$ is a very small positive constant.

It is clear from Eq. (2.1) that the suction velocity at the plate surface is a function time only. Assuming that, the suction velocity takes the following exponential form:

$$v = -V_o \left[1 + \varepsilon A \exp\left(int\right)\right] \tag{2.6}$$

where A is a real positive constant, ε and εA are small less than unity. V_o is a scale of suction velocity which is non-zero positive constant, the negative sign indicates that the suction is towards the plate.

Following Magyari and Pantokratoras [34], Venkateswarlu et al. [35] by using the Rosseland approximation, the radiative flux vector q_r can be written as:

$$\frac{\partial q_r}{\partial y} = -\frac{4\sigma^*}{3a^*}\frac{\partial T^4}{\partial y} \tag{2.7}$$

where, σ^* and a^* are the Stefan-Boltzmann constant and the mean absorption coefficient respectively. We assume that the difference between fluid temperature T and cold wall temperature T_o within the flow is sufficiently small such that T^4 may be expressed as a linear function of the temperature. This is accomplished by expanding T^4 in Taylor series about the cold wall temperature T_o and neglecting the second and higher order terms, we have

$$T^4 \cong 4T_o^3 T - 3T_o^4 \tag{2.8}$$

Using equations (2.7) and (2.8) in equation (2.3) we obtain

$$\frac{\partial T}{\partial t} + v\frac{\partial T}{\partial y} = \frac{K_T}{\rho c_p}\left[1 + \frac{16\sigma^* T_o^3}{3a^* K_T}\right]\frac{\partial^2 T}{\partial y^2} - \frac{Q_o}{\rho c_p}\left(T - T_0\right) + \frac{Q_1}{\rho c_p}\left(C - C_0\right) + \frac{D_m K_T}{c_s c_p}\frac{\partial^2 C}{\partial y^2} \tag{2.9}$$

We introduce the following non-dimensional variables

$$\left.\begin{array}{l} \xi = \frac{x}{h}, \quad \eta = \frac{y}{h}, \quad \psi = \frac{h}{\nu}u, \quad P = \frac{h^2}{\rho\nu^2}p, \quad \gamma = \frac{\phi_1}{h}, \quad \sigma = \frac{\phi_2}{h}, \\ \omega = \frac{h^2}{v}n, \quad \tau = \frac{v}{h^2}t, v = hV_o, \quad \theta = \frac{T - T_o}{T_1 - T_o}, \quad \phi = \frac{C - C_o}{C_1 - C_o}. \end{array}\right\} \tag{2.10}$$

Equations (2.2), (2.4) and (2.9) reduce to the following non-dimensional form

$$\frac{\partial \psi}{\partial \tau} - \left[1 + \varepsilon A e^{i\omega\tau}\right]\frac{\partial \psi}{\partial \eta} = -\frac{dP}{d\xi} + \frac{\partial^2 \psi}{\partial \eta^2} + Gr\theta + Gm\phi - \left[M + \frac{1}{Da}\right]\psi \tag{2.11}$$

$$\frac{\partial \theta}{\partial \tau} - \left[1 + \varepsilon A e^{i\omega\tau}\right]\frac{\partial \theta}{\partial \eta} = \left[\frac{1 + N}{\mathrm{Pr}}\right]\frac{\partial^2 \theta}{\partial \eta^2} - H\theta + Du\frac{\partial^2 \phi}{\partial \eta^2} + Q\phi \tag{2.12}$$

$$\frac{\partial \phi}{\partial \tau} - \left[1 + \varepsilon A e^{i\omega\tau}\right]\frac{\partial \phi}{\partial \eta} = \frac{1}{Sc}\frac{\partial^2 \phi}{\partial \eta^2} - Kr\phi \tag{2.13}$$

Here $Gr = \frac{g\beta_T(T_1 - T_o)h^3}{v^2}$ is the thermal buoyancy force, $Gm = \frac{g\beta_C(C_1 - C_0)h^3}{v^2}$ is the concentration buoyancy force, $M = \frac{\sigma_e B_o^2 h^2}{\rho v}$ is the magnetic parameter, $Da = \frac{K}{h^2}$ is the Darcy parameter, $\mathrm{Pr} = \frac{\rho c_p \nu}{K_T}$ is the Prandtl number, $N = \frac{16\sigma^* T_o^3}{3a^* K_T}$ is the thermal radiation parameter, $Du = \frac{D_m(C_1 - C_o)K_T}{c_s c_p(T_1 - T_o)\nu}$ is the Dufour number, $H = \frac{Q_0 h^2}{\rho c_p \nu}$ is the heat source parameter,

$Q = \frac{Q_1(C_1-C_o)h^2}{\rho c_p(T_1-T_o)\nu}$ is the absorption of radiation parameter, $Sc = \frac{\nu}{D_m}$ is the Schmidt number and $Kr = \frac{h^2}{\nu}K_r^*$ is the chemical reaction parameter respectively.

The corresponding initial and boundary conditions in Eq. (2.5) in non-dimensional form are

$$\left.\begin{array}{l} \psi = \gamma\psi', \quad \theta = 0, \quad \phi = 0 \text{ at } \eta = 0 \\ \psi = \sigma\psi', \quad \theta = 1 + \varepsilon\exp(i\omega\tau), \quad \phi = 1 + \varepsilon\exp(i\omega\tau) \quad \text{at} \quad \eta = 1 \end{array}\right\} \tag{2.14}$$

Following Adesanya and Makinde [36], for purely an oscillatory flow we take the pressure gradient of the form

$$\lambda = -\frac{dP}{d\xi} = \lambda_0 + \varepsilon\exp(i\omega\tau)\lambda_1 \tag{2.15}$$

where λ_0- and λ_1- are constants and ω is the frequency of oscillation.

It is now important to calculate physical quantities of primary interest, which are the local wall shear stress or skin friction coefficient, the local surface heat flux and the local surface mass flux. Given the velocity, temperature and concentration fields in the boundary layer, the shear stress τ_w, the heat flux q_w and mass flux j_w are obtained by

$$\tau_w = \mu\left[\frac{\partial u}{\partial y}\right] \tag{2.16}$$

$$q_w = -K_T\left[\frac{\partial T}{\partial y}\right] \tag{2.17}$$

$$j_w = -D_m\left[\frac{\partial C}{\partial y}\right] \tag{2.18}$$

In non-dimensional form the skin-friction coefficient Cf, heat transfer coefficient Nu and mass transfer coefficient Sh are defined as

$$Cf = \frac{\tau_w}{\rho(\nu/h)^2} \tag{2.19}$$

$$Nu = \frac{hq_w}{K_T(T_1 - T_o)} \tag{2.20}$$

$$Sh = \frac{hj_w}{D_m(C_1 - C_o)} \tag{2.21}$$

Using non-dimensional variables in equation (2.10) and equations (2.16) to (2.18) into equations (2.19) to (2.21), we obtain the physical parameters

$$Cf = \left[\frac{\partial\psi}{\partial\eta}\right] \tag{2.22}$$

$$Nu = -\left[\frac{\partial\theta}{\partial\eta}\right] \tag{2.23}$$

$$Sh = -\left[\frac{\partial\phi}{\partial\eta}\right] \tag{2.24}$$

3. SOLUTION OF THE PROBLEM

Equations (2.11) to (2.13) are coupled non-linear partial differential equations and these cannot be solved in closed form. So, we reduce these non-linear partial differential equations into a set of ordinary differential equations, which can be solved analytically. This can be done by assuming the trial solutions for the velocity, temperature and concentration of the fluid as (see, Siva Kumar et al. [37], Venkateswarlu et al. [38])

$$\psi(\eta,\tau) = \psi_0(\eta) + \varepsilon \exp(i\omega\tau)\,\psi_1(\eta) + o\left(\varepsilon^2\right) \tag{3.1}$$

$$\theta(\eta,\tau) = \theta_0(\eta) + \varepsilon \exp(i\omega\tau)\,\theta_1(\eta) + o\left(\varepsilon^2\right) \tag{3.2}$$

$$\phi(\eta,\tau) = \phi_0(\eta) + \varepsilon \exp(i\omega\tau)\,\phi_1(\eta) + o\left(\varepsilon^2\right) \tag{3.3}$$

Substituting equations (3.1) to (3.3) into equations (2.11) to (2.13), then equating the harmonic and non–harmonic terms and neglecting the higher order terms of $o\left(\varepsilon^2\right)$, we obtain

$$\psi_0'' + \psi_0' - \left[M + \frac{1}{Da}\right]\psi_0 = -\left[Gr\theta_0 + Gm\phi_0 + \lambda_0\right] \tag{3.4}$$

$$\psi_1'' + \psi_1' - \left[M + \frac{1}{Da} + i\omega\right]\psi_1 = -\left[Gr\theta_1 + Gm\phi_1 + \lambda_1 + A\psi_0'\right] \tag{3.5}$$

$$\theta_0'' + \left[\frac{\Pr}{1+N}\right]\theta_0' - \left[\frac{H\Pr}{1+N}\right]\theta_0 = -\left[\frac{\Pr Du}{1+N}\phi_0'' + \frac{\Pr Q}{1+N}\phi_0\right] \tag{3.6}$$

$$\theta_1'' + \left[\frac{\Pr}{1+N}\right]\theta_1' - \left[\frac{\Pr(H+i\omega)}{1+N}\right]\theta_1 = -\left[\frac{\Pr Du}{1+N}\phi_1'' + \frac{\Pr Q}{1+N}\phi_1 + \frac{\Pr A}{1+N}\theta_0'\right] \tag{3.7}$$

$$\phi_0'' + Sc\phi_0' - ScKr\phi_0 = 0 \tag{3.8}$$

$$\phi_1'' + Sc\phi_1' - Sc(Kr + i\omega)\phi_1 = -ScA\phi_0' \tag{3.9}$$

Initial and boundary conditions, presented by equation (2.14), can be written as

$$\left.\begin{array}{llllllll} \psi_0 = \gamma\psi_0', & \psi_1 = \gamma\psi_1', & \theta_o = 0, & \theta_1 = 0, & \phi_o = 0, & \phi_1 = 0 & \text{at} & \eta = 0 \\ \psi_o = \sigma\psi_0', & \psi_1 = \sigma\psi_1', & \theta_o = 1, & \theta_1 = 1, & \phi_o = 1, & \phi_1 = 1 & \text{at} & \eta = 1 \end{array}\right\} \tag{3.10}$$

where the prime denotes ordinary differentiation with respect toη.

The analytical solutions of equations (3.4) to (3.9) with the boundary conditions in equation (3.10), are given by

$$\begin{aligned}\psi_0 =& C_{22}\exp(-m_9\eta) + C_{21}\exp(m_{10}\eta) - C_3\exp(-m_5\eta) - C_4\exp(m_6\eta) \\ &+ C_5\exp(-m_1\eta) + C_6\exp(m_2\eta) + C_2\end{aligned} \tag{3.11}$$

$$\begin{aligned}\psi_1 =& D_{54}\exp(-m_{11}\eta) + D_{53}\exp(m_{12}\eta) - D_{23}\exp(-m_1\eta) - D_{24}\exp(m_2\eta) \\ &+ D_{25}\exp(-m_3\eta) + D_{26}\exp(m_4\eta) - D_{27}\exp(-m_5\eta) + D_{28}\exp(m_6\eta) \\ &- D_{29}\exp(-m_7\eta) - D_{30}\exp(m_8\eta) + D_{31}\exp(-m_9\eta) - D_{32}\exp(m_{10}\eta) + D_{12}\end{aligned} \tag{3.12}$$

$$\theta_o = B_{14}\exp(-m_5\eta) + B_{13}\exp(m_6\eta) + B_7\exp(-m_1\eta) - B_8\exp(m_2\eta) \tag{3.13}$$

$$\theta_1 = B_{50}\exp(-m_7\eta) + B_{47}\exp(m_8\eta) - B_{31}\exp(-m_3\eta) - B_{32}\exp(m_4\eta)$$

$$+ B_{33}\exp(m_2\eta) + B_{34}\exp(-m_1\eta) + B_{35}\exp(-m_5\eta) - B_{36}\exp(m_6\eta) \quad (3.14)$$

$$\phi_o = A_1\exp(m_2\eta) - A_1\exp(-m_1\eta) \quad (3.15)$$

$$\phi_1 = A_{14}\exp(-m_3\eta) + A_{13}\exp(m_4\eta) - A_7\exp(m_2\eta) - A_8\exp(-m_1\eta) \quad (3.16)$$

By substituting equations (3.11) to (3.16) into equations (3.1) to (3.3), we obtained solutions for the fluid velocity, temperature and concentration and are presented in the following form

$$\begin{aligned}\psi(\eta,\tau) =&[C_{22}\exp(-m_9\eta) + C_{21}\exp(m_{10}\eta) - C_3\exp(-m_5\eta) - C_4\exp(m_6\eta)\\ &+ C_5\exp(-m_1\eta) + C_6\exp(m_2\eta) + C_2]\\ &+ \varepsilon\exp(i\omega\tau)[D_{54}\exp(-m_{11}\eta) + D_{53}\exp(m_{12}\eta) - D_{23}\exp(-m_1\eta)\\ &- D_{24}\exp(m_2\eta) + D_{25}\exp(-m_3\eta) + D_{26}\exp(m_4\eta)\\ &- D_{27}\exp(-m_5\eta) + D_{28}\exp(m_6\eta) - D_{29}\exp(-m_7\eta)\\ &- D_{30}\exp(m_8\eta) + D_{31}\exp(-m_9\eta) - D_{32}\exp(m_{10}\eta) + D_{12}]\end{aligned} \quad (3.17)$$

$$\begin{aligned}\theta(\eta,\tau) =& [B_{14}\exp(-m_5\eta) + B_{13}\exp(m_6\eta) + B_7\exp(-m_1\eta) - B_8\exp(m_2\eta)]\\ &+ \varepsilon\exp(i\omega\tau)[B_{50}\exp(-m_7\eta) + B_{47}\exp(m_8\eta) - B_{31}\exp(-m_3\eta)\\ &- B_{32}\exp(m_4\eta) + B_{33}\exp(m_2\eta) + B_{34}\exp(-m_1\eta) + B_{35}\exp(-m_5\eta)\\ &- B_{36}\exp(m_6\eta)]\end{aligned} \quad (3.18)$$

$$\begin{aligned}\phi(\eta,\tau) =&[A_1\exp(m_2\eta) - A_1\exp(-m_1\eta)] + \varepsilon\exp(i\omega\tau)[A_{14}\exp(-m_3\eta)\\ &+ A_{13}\exp(m_4\eta) - A_7\exp(m_2\eta) - A_8\exp(-m_1\eta)]\end{aligned} \quad (3.19)$$

3.1. **Skin friction:** From the velocity field, the skin friction at the plate can be obtained, which in non dimensional form is given by

$$\begin{aligned}Cf =&[C_{21}m_{10}\exp(m_{10}\eta) - C_{22}m_9\exp(-m_9\eta) + C_3m_5\exp(-m_5\eta)\\ &- C_4m_6\exp(m_6\eta) + C_6m_2\exp(m_2\eta) - C_5m_1\exp(-m_1\eta)]\\ &+ \varepsilon\exp(i\omega\tau)[D_{53}m_{12}\exp(m_{12}\eta) - D_{54}m_{11}\exp(-m_{11}\eta)\\ &+ D_{23}m_1\exp(-m_1\eta) - D_{24}m_2\exp(m_2\eta) + D_{26}m_4\exp(m_4\eta)\\ &- D_{25}m_3\exp(-m_3\eta) + D_{27}m_5\exp(-m_5\eta) + D_{28}m_6\exp(m_6\eta)\\ &+ D_{29}m_7\exp(-m_7\eta) - D_{30}m_8\exp(m_8\eta) - D_{31}m_9\exp(-m_9\eta)\\ &- D_{32}m_{10}\exp(m_{10}\eta)]\end{aligned} \quad (3.20)$$

3.2. **Nusselt number:** From temperature field, we obtained heat transfer coefficient which is given in non-dimensional form as

$$\begin{aligned}Nu =& -[B_{13}m_6\exp(m_6\eta) - B_{14}m_5\exp(-m_5\eta) - B_7m_1\exp(-m_1\eta)\\ &- B_8m_2\exp(m_2\eta)] - \varepsilon\exp(i\omega\tau)[B_{47}m_8\exp(m_8\eta) - B_{50}m_7\exp(-m_7\eta)\\ &+ B_{31}m_3\exp(-m_3\eta) - B_{32}m_4\exp(m_4\eta) + B_{33}m_2\exp(m_2\eta)\\ &- B_{34}m_1\exp(-m_1\eta) - B_{35}m_5\exp(-m_5\eta) - B_{36}m_6\exp(m_6\eta)]\end{aligned} \quad (3.21)$$

3.3. **Sherwood number:** From concentration field, we obtained mass transfer coefficient which is given in non-dimensional form as

$$Sh = -\left[A_1 m_1 \exp\left(-m_1\eta\right) + A_1 m_2 \exp\left(m_2\eta\right)\right] - \varepsilon \exp\left(i\omega\tau\right)\left[A_{13} m_4 \exp\left(m_4\eta\right)\right.$$
$$\left. - A_{14} m_3 \exp\left(-m_3\eta\right) - A_7 m_2 \exp\left(m_2\eta\right) + A_8 m_1 \exp\left(-m_1\eta\right)\right] \tag{3.22}$$

Here the constants are not given under brevity.

4. Results and discussion

The results are obtained to illustrate the influence of the thermal Grashof number Gr, solutal Grashof number Gm, Darcy parameter Da, pressure gradient λ, magnetic parameter M, Prandtl number Pr, heat source parameter H, radiation parameter N, absorption of radiation parameter Q, Dufour number Du, Schmidt number Sc, chemical reaction parameter Kr, cold wall slip parameter γ and heated wall slip parameter σ on the fluid velocity ψ, temperature θ and concentration ϕ. The numerical values of skin friction coefficient Cf, heat transfer coefficient Nu and mass transfer coefficient Sh are presented in tabular form for various values of different physical parameters. For graphical results and tables we considered $\tau = \pi/2, Gr = 5, Gm = 3, M = 4, Da = 1, \mathrm{Pr} = 0.71, N = 0.2, H = 0.5, Sc = 0.60, Du = 0.4, \lambda = 1, Kr = 0.5, Q = 0.3, A = 0.1, \gamma = 0.1, \sigma = 0.1, \omega = 1,$ and $\varepsilon = 0.00001$.

These values are kept as common in entire study except the varied values as shown in respective graph and table.

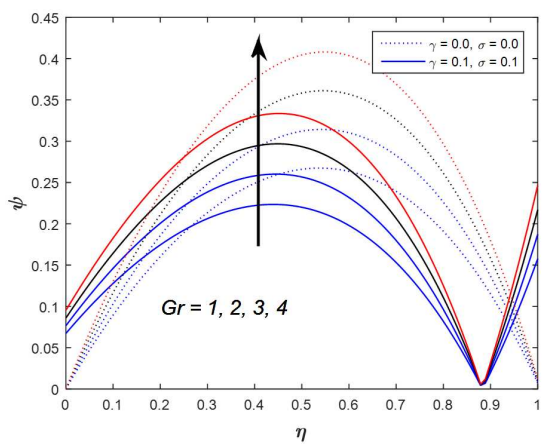

FIGURE 2. Velocity for various values of thermal Grashof number under the slip and no-slip boundary conditions.

Figs. 2 and 3 show the influence of the thermal buoyancy force parameter Gr and solutal buoyancy force parameter Gm on the fluid velocity profile ψ respectively. A study of the curves shows that thermal buoyancy force parameter Gr and solutal buoyancy force parameter Gm accelerates the fluid velocity under the slip and no-slip boundary conditions. This is due to

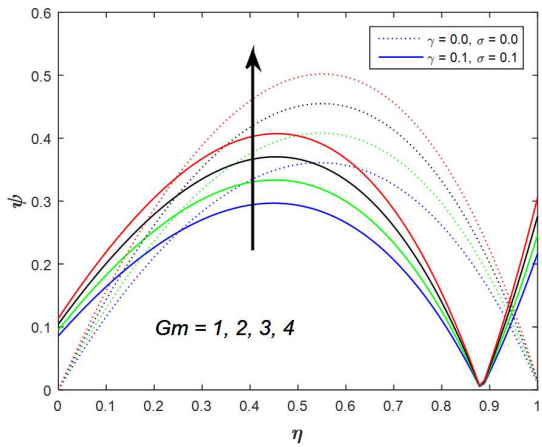

FIGURE 3. Velocity for various values of solutal Grashof number under the slip and no-slip boundary conditions.

the fact that buoyancy force enhances fluid velocity and increase the boundary layer thickness with increase in the value of Gr or Gm.

The variation of fluid velocity profile ψ with Darcy parameter Da is represented in Fig. 4 under the slip and no-slip boundary conditions. This figure clearly indicates that the value of velocity profile increases with increasing the Darcy parameter except at the flow reversal point at the heated wall.

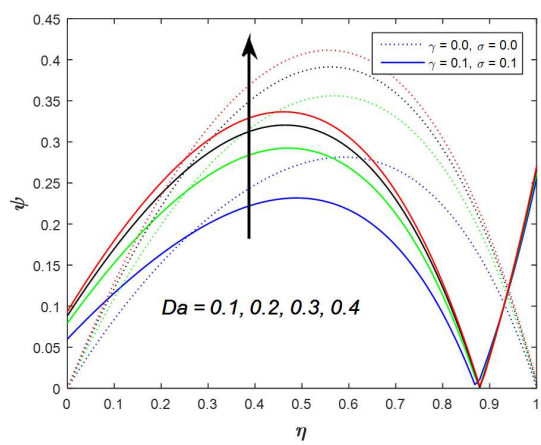

FIGURE 4. Velocity for various values of Darcy parameter under the slip and no-slip boundary conditions.

Fig.5 demonstrates the influence of pressure gradient λ on the fluid velocity ψ. It is observed that, the fluid velocity increases on increasing the pressure gradient under the slip and no-slip boundary conditions.

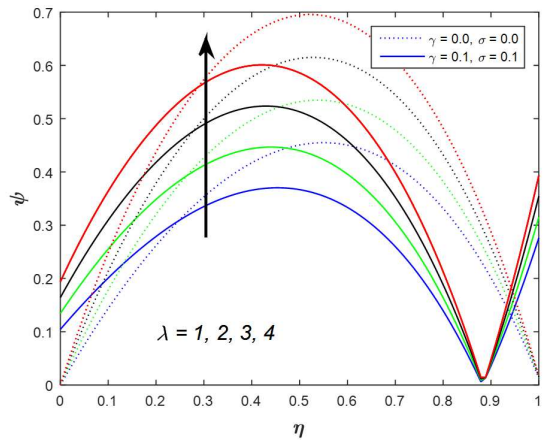

FIGURE 5. Velocity for various values of pressure gradient under the slip and no-slip boundary conditions.

Figs. 6 and 7, shows the plot of fluid velocity ψ and temperature θ of the flow field against different values of Prandtl number Pr taking other parameters are constant. The Prandtl number defines the ratio of momentum diffusivity to thermal diffusivity. It is evident from Fig. 6, the fluid velocity increases on increasing Prandtl number Pr under the slip and no-slip boundary conditions. It is clear that from Fig. 7, temperature increases on increasing Prandtl number.

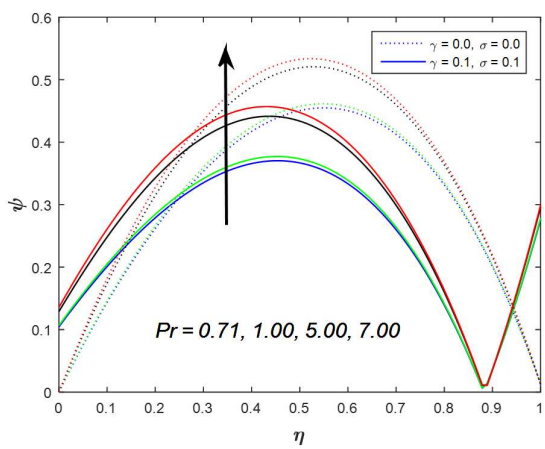

FIGURE 6. Velocity for various values of Prandtl number under the slip and no-slip boundary conditions.

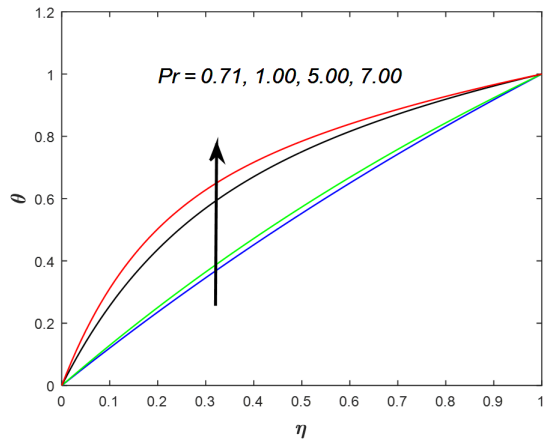

FIGURE 7. Temperature for various values of Prandtl number.

Figs. 8 and 9, show the influence of the heat source parameter H and absorption of radiation parameter Q on the fluid velocity profile ψ respectively under the slip and no-slip boundary conditions. The effect of increasing the value of the heat source parameter is to decrease the boundary layer as shown in Fig. 8, which is as expected due to the fact that when heat is absorbed the buoyancy force decreases which retards the flow rate and thereby giving rise to decrease in the velocity profiles. The opposite trend is observed for the case of increasing the value of the absorption of the radiation parameter due to increase in the buoyancy force which accelerates the flow rate as shown in Fig. 9.

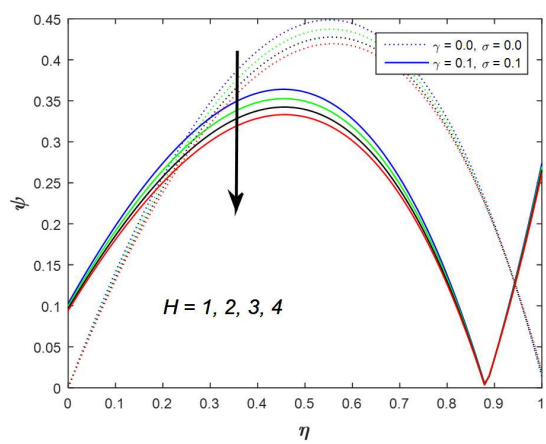

FIGURE 8. Velocity for various values of heat source parameter under the slip and no-slip boundary conditions.

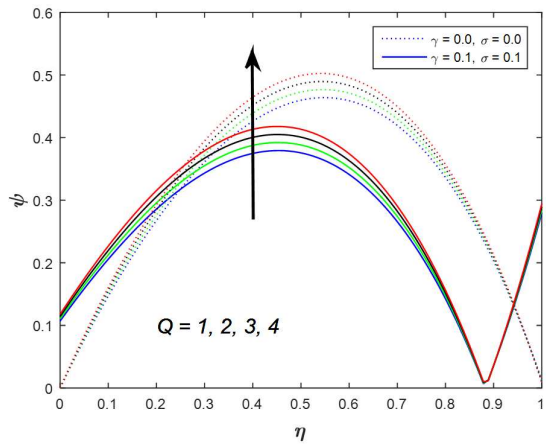

FIGURE 9. Velocity for various values of absorption of radiation parameter under the slip and no-slip boundary conditions.

Fig. 10 depicts the influence of magnetic field intensity on the variation of fluid velocity under the slip and no-slip boundary conditions. It is noticed that, an increase in the magnetic parameter M decreases the fluid velocity ψ due to the resistive action of the Lorenz forces except at the heated wall where the reversed flow induced by wall slip caused an increase in the fluid velocity. This implies that magnetic field tends to decelerate fluid flow under the slip and no-slip boundary conditions.

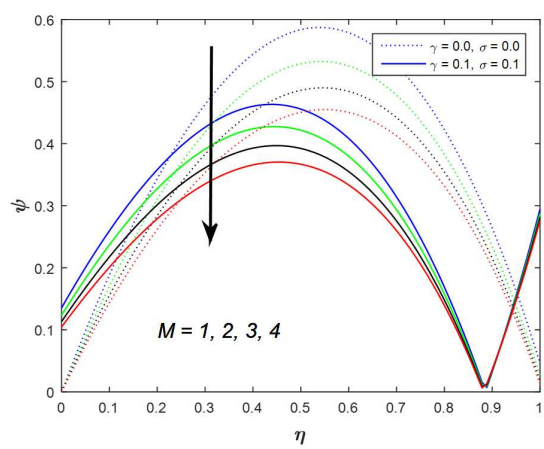

FIGURE 10. Velocity for various values of magnetic parameter under the slip and no-slip boundary conditions.

The variation of fluid velocity profile ψ with radiation parameter N is represented in Fig. 11 under the slip and no-slip boundary conditions. It is observed that, the fluid velocity decreases on increasing the radiation parameter.

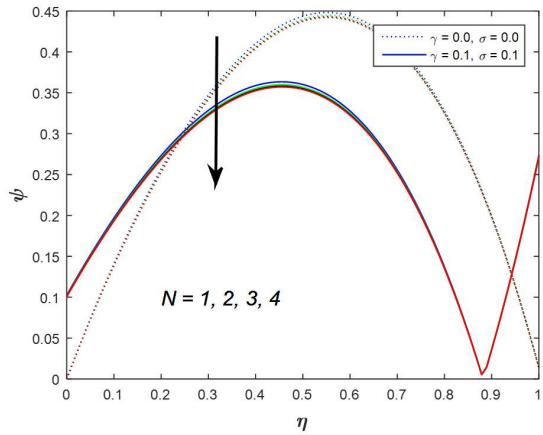

FIGURE 11. Velocity for various values of radiation parameter under the slip and no-slip boundary conditions.

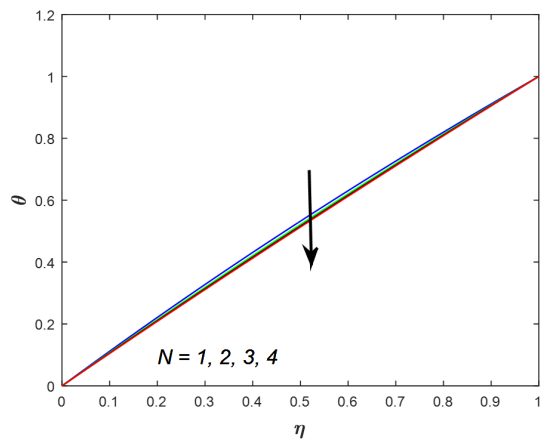

FIGURE 12. Temperature for various values of radiation parameter.

Fig. 12 represents graph of fluid temperature distribution θ with span wise co-ordinate η for different values of radiation parameter N. It is observed from this figure that increase in the radiation parameter decreases the temperature distribution in the thermal boundary layer due to decrease in the thickness of the thermal boundary layer with thermal radiation parameter. This is because large values of radiation parameter correspond to an increase in dominance

of conduction over radiation, thereby decreasing the buoyancy force and the thickness of the thermal boundary layer.

The influence of Dufour number for different values on velocity and temperature profiles are plotted in Figs. 13 and 14 respectively. The Dufour number signifies the contribution of the concentration gradient to the thermal energy flux in the flow. It is found that an increase in the Dufour number Du causes a decrease in velocity ψ under the slip and no-slip boundary conditions. It is found that, the fluid temperature θ decreases on increasing the Dufour number Du.

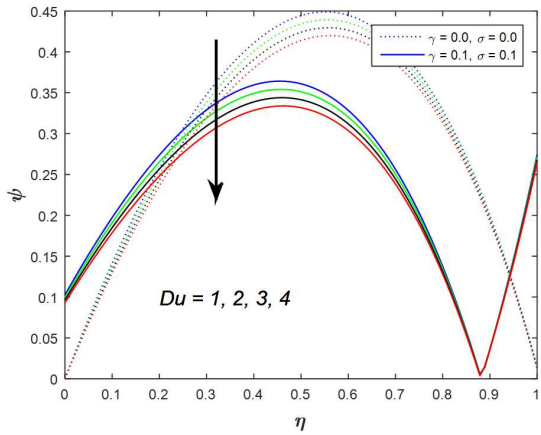

FIGURE 13. Velocity for various values of Dufour number under the slip and no-slip boundary conditions.

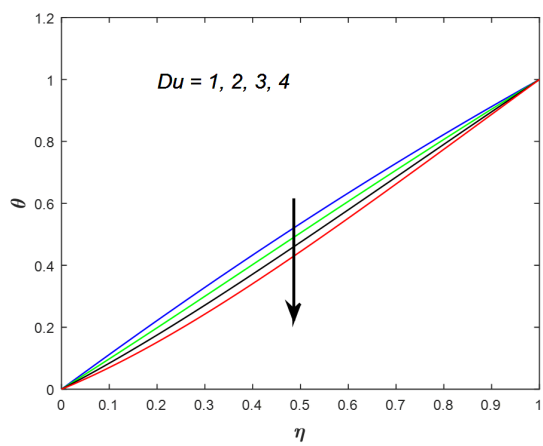

FIGURE 14. Temperature for various values of Dufour number.

Fig. 15 has been plotted to depict the variation of temperature profiles for different values of heat source parameter by fixing other physical parameters. From this graph we observe that temperature θ decreases with increase in the heat source parameter H because when heat is absorbed, the buoyancy force decreases the temperature profile.

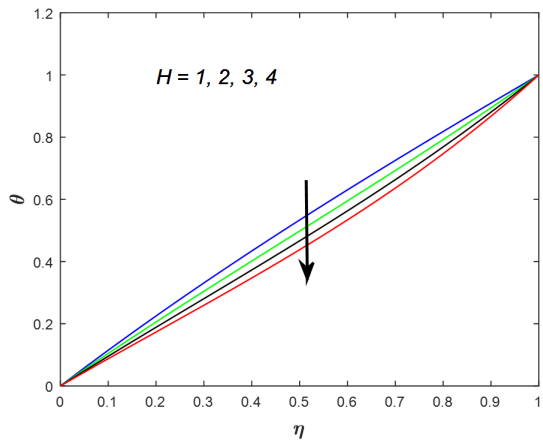

FIGURE 15. Temperature for various values of heat source parameter.

Fig. 16 depicts the graph of temperature profile for various values of absorption of radiation parameter in the boundary layer. It is seen that the effect of absorption of radiation parameter Q is to increase temperature θ in the boundary layer as the radiated heat is absorbed by the fluid which is responsible for increase in the temperature of the fluid very close to the porous boundary layer.

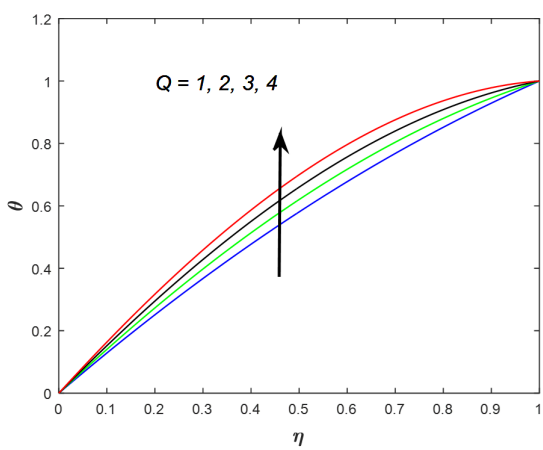

FIGURE 16. Temperature for various values of absorption of radiation parameter.

The nature of the fluid velocity, temperature and concentration is shown in Figs. 17 to 19. Physically, Schmidt number signifies the relative strength of viscosity to chemical molecular diffusivity. Therefore the Schmidt number quantifies the relative effectiveness of momentum and mass transport by diffusion in the hydrodynamic and concentration boundary layers. It is observed that velocity ψ increases on increasing the Schmidt number Sc under the slip and no-slip boundary conditions and temperature θ decreases on increasing Schmidt number Sc whereas concentration ϕ increases on increasing the Schmidt number Sc.

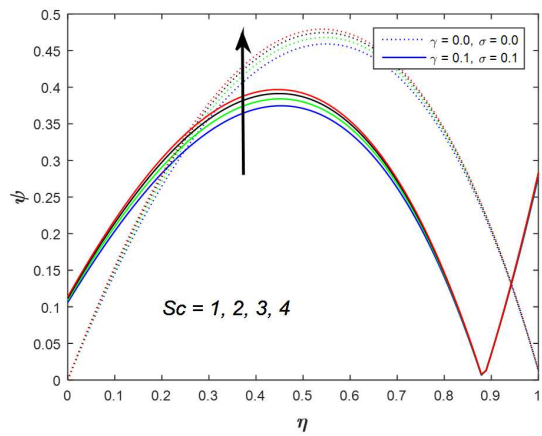

FIGURE 17. Velocity for various values of Schmidt number under the slip and no-slip boundary conditions.

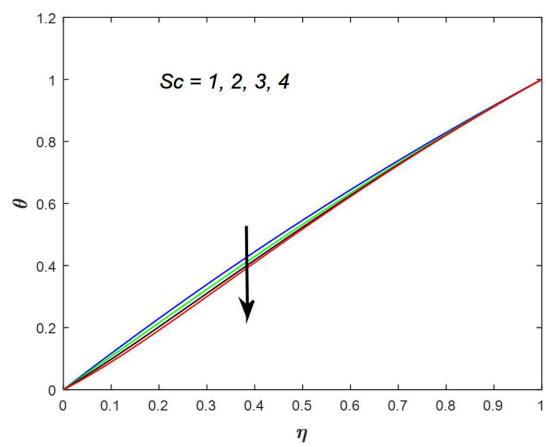

FIGURE 18. Temperature for various values of Schmidt number.

Figs. 20 to 22, demonstrate the influence of chemical reaction parameter Kr on the velocity, temperature and species concentration. It is observed that, velocity ψ decreases on increasing

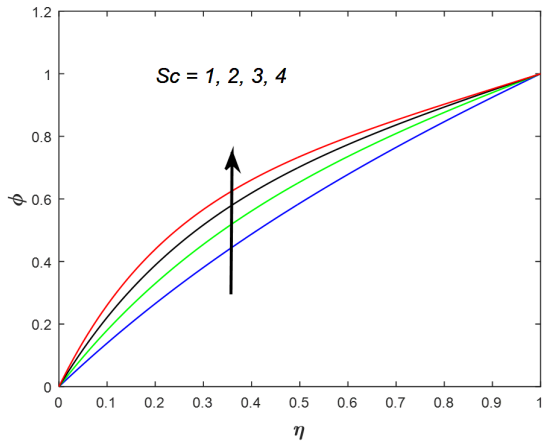

FIGURE 19. Concentration for various values of Schmidt number.

the chemical reaction parameter Kr under the slip and no-slip boundary conditions. It also found that, temperature θ increases and concentration ϕ decreases on increasing the chemical reaction parameter Kr. This implies that, chemical reaction tends to reduce the fluid velocity and species concentration.

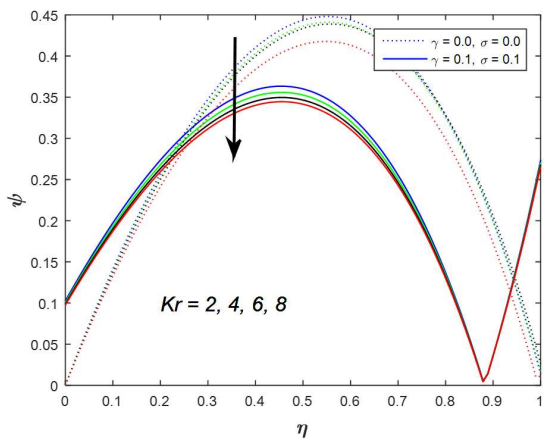

FIGURE 20. Velocity for various values of chemical reaction parameter under the slip and no-slip boundary conditions.

Figs. 23 and 24 shows the fluid velocity profile variations with the cold wall slip parameter γ and the heated wall slip parameter σ. It is observed that, the fluid velocity ψ increases on increasing the cold wall slip parameter γ thus enhancing the fluid flow. The cold wall slip parameter did not cause an appreciable effect on the heated wall. An increase in the heated wall slip parameter σ decreases the fluid velocity ψ minimally at the cold wall and increasing

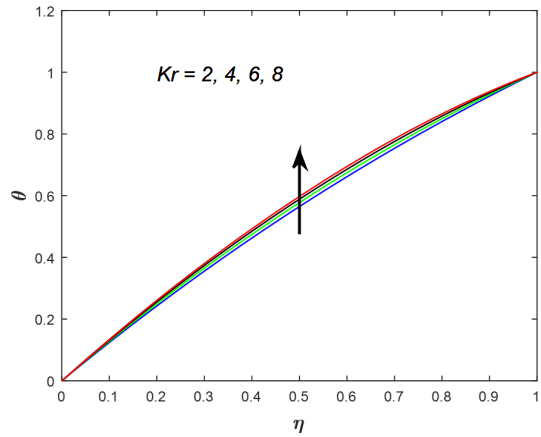

FIGURE 21. Temperature for various values of chemical reaction parameter.

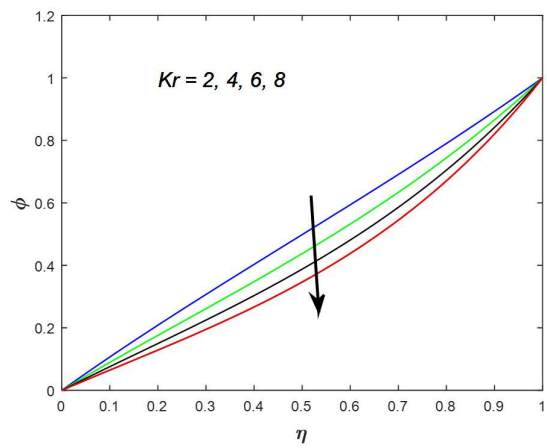

FIGURE 22. Concentration for various values of chemical reaction parameter.

the heated wall slip parameter σ causes a flow reversal towards the heated wall. It is observed that $\sigma = 0$ corresponds to the pulsatile case with no slip condition at the heated wall in Fig 24.

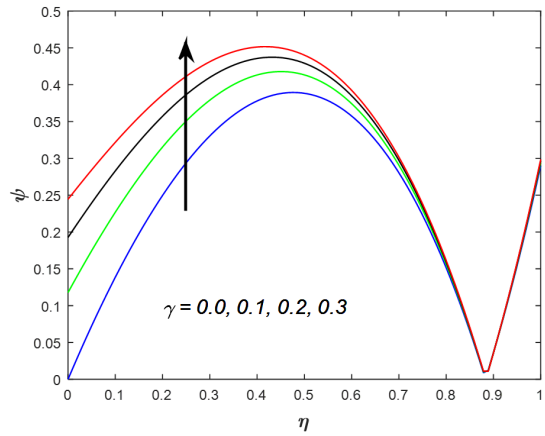

FIGURE 23. Velocity for various values of cold wall slip parameter.

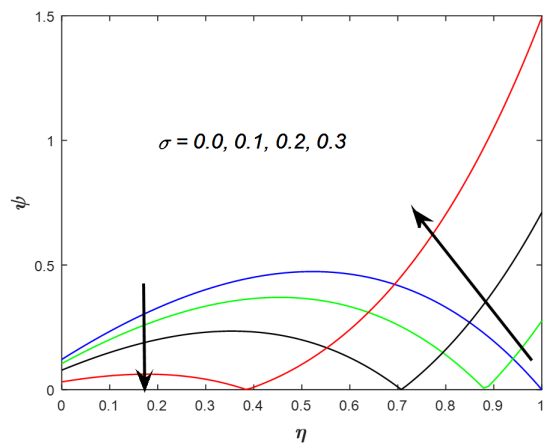

FIGURE 24. Velocity for various values of heated wall slip parameter.

From tables 1 to 12, it is clear that the skin friction coefficient Cfincreases on increasing the thermal Grashof number Gr, solutal Grashof number Gm, pressure gradient λ, Darcy parameter Da, Prandtl number Pr, absorption of radiation parameter Q and Schmidt number Sc whereas it decreases on increasing magnetic parameter M, radiation parameter N, heat source parameter H, Dufour number Du and chemical reaction parameter Kr at both cold and heated walls.

TABLE 1. Influence of thermal Grashof number on skin friction coefficient.

η	Gr	Cf	Gr	Cf	Gr	Cf	Gr	Cf
0.00	1.0	0.6728	2.0	0.7660	3.0	0.8592	4.0	0.9524
0.25	1.0	0.3190	2.0	0.3800	3.0	0.4410	4.0	0.5020
0.50	1.0	0.1161	2.0	0.1253	3.0	0.1345	4.0	0.1438
0.75	1.0	0.7104	2.0	0.8331	3.0	0.9558	4.0	1.0786
1.00	1.0	1.5768	2.0	1.8733	3.0	2.1698	4.0	2.4663

TABLE 2. Influence of Solutal Grashof number on skin friction coefficient.

η	Gm	Cf	Gm	Cf	Gm	Cf	Gm	Cf
0.00	1.0	0.8581	2.0	0.9518	3.0	1.0456	4.0	1.1393
0.25	1.0	0.4410	2.0	0.5020	3.0	0.5631	4.0	0.6241
0.50	1.0	0.1338	2.0	0.1434	3.0	0.1530	4.0	0.1626
0.75	1.0	0.9556	2.0	1.0784	3.0	1.2013	4.0	1.3241
1.00	1.0	2.1702	2.0	2.4665	3.0	2.7628	4.0	3.0591

TABLE 3. Influence of magnetic parameter on skin friction coefficient.

η	M	Cf	M	Cf	M	Cf	M	Cf
0.00	1.0	1.3544	2.0	1.2349	3.0	1.1331	4.0	1.0456
0.25	1.0	0.6847	2.0	0.6384	3.0	0.5983	4.0	0.5631
0.50	1.0	0.2527	2.0	0.2135	3.0	0.1807	4.0	0.1530
0.75	1.0	1.4512	2.0	1.3554	3.0	1.2730	4.0	1.2013
1.00	1.0	2.9448	2.0	2.8733	3.0	2.8133	4.0	2.7628

TABLE 4. Influence of pressure gradient on skin friction coefficient.

η	λ	Cf	λ	Cf	λ	Cf	λ	Cf
0.00	1.0	1.0456	2.0	1.3440	3.0	1.6424	4.0	1.9408
0.25	1.0	0.5631	2.0	0.6379	3.0	0.7128	4.0	0.7876
0.50	1.0	0.1530	2.0	0.2310	3.0	0.3090	4.0	0.3871
0.75	1.0	1.2013	2.0	1.4205	3.0	1.6397	4.0	1.8589
1.00	1.0	2.7628	2.0	3.1541	3.0	3.5455	4.0	3.9368

It is evident from tables 13 and 14 that skin friction coefficient decreases at the cold wall and it increases at the heated wall on increasing the cold wall slip parameter γ and heated wall slip parameter σ.

TABLE 5. Influence of Darcy parameter on skin friction coefficient.

η	Da	Cf	Da	Cf	Da	Cf	Da	Cf
0.00	0.1	0.5998	0.2	0.7918	0.3	0.8824	0.4	0.9351
0.25	0.1	0.3701	0.2	0.4567	0.3	0.4956	0.4	0.5177
0.50	0.1	0.0247	0.2	0.0766	0.3	0.1031	0.4	0.1190
0.75	0.1	0.8211	0.2	0.9884	0.3	1.0654	0.4	1.1096
1.00	0.1	2.5481	0.2	2.6266	0.3	2.6728	0.4	2.7011

TABLE 6. Influence of Prandtl number on skin friction coefficient.

η	Pr	Cf	Pr	Cf	Pr	Cf	Pr	Cf
0.00	0.71	1.0456	1.00	1.0663	5.00	1.2901	7.00	1.3575
0.25	0.71	0.5631	1.00	0.5728	5.00	0.6493	7.00	0.6584
0.50	0.71	0.1530	1.00	0.1598	5.00	0.2460	7.00	0.2747
0.75	0.71	1.2013	1.00	1.2202	5.00	1.3888	7.00	1.4244
1.00	0.71	2.7628	1.00	2.7848	5.00	2.9621	7.00	2.9947

TABLE 7. Influence of radiation parameter on skin friction coefficient.

η	N	Cf	N	Cf	N	Cf	N	Cf
0.00	1.0	1.0249	2.0	1.0145	3.0	1.0093	4.0	1.0061
0.25	1.0	0.5530	2.0	0.5478	3.0	0.5452	4.0	0.5436
0.50	1.0	0.1465	2.0	0.1434	3.0	0.1418	4.0	0.1409
0.75	1.0	1.1819	2.0	1.1719	3.0	1.1669	4.0	1.1638
1.00	1.0	2.7399	2.0	2.7280	3.0	2.7219	4.0	2.7182

TABLE 8. Influence of heat source parameter on skin friction coefficient.

η	H	Cf	H	Cf	H	Cf	H	Cf
0.00	1.0	1.0283	2.0	0.9966	3.0	0.9684	4.0	0.9430
0.25	1.0	0.5532	2.0	0.5351	3.0	0.5188	4.0	0.5041
0.50	1.0	0.1487	2.0	0.1410	3.0	0.1343	4.0	0.1285
0.75	1.0	1.1829	2.0	1.1491	3.0	1.1188	4.0	1.0913
1.00	1.0	2.7392	2.0	2.6955	3.0	2.6558	4.0	2.6196

From table 15 to 18, it is clear that the heat transfer coefficient Nu increases at the cold wall and decreases at the heated wall on increasing the radiation parameter N, heat source parameter H, Dufour number Du and Schmidt number Sc.

TABLE 9. Influence of Dufour number on skin friction coefficient.

η	Du	Cf	Du	Cf	Du	Cf	Du	Cf
0.00	1.0	1.0265	2.0	0.9948	3.0	0.9631	4.0	0.9314
0.25	1.0	0.5545	2.0	0.5401	3.0	0.5258	4.0	0.5115
0.50	1.0	0.1466	2.0	0.1358	3.0	0.1251	4.0	0.1143
0.75	1.0	1.1843	2.0	1.1561	3.0	1.1279	4.0	1.0997
1.00	1.0	2.7436	2.0	2.7115	3.0	2.6795	4.0	2.6475

TABLE 10. Influence of absorption of radiation parameter on skin friction coefficient.

η	Q	Cf	Q	Cf	Q	Cf	Q	Cf
0.00	1.0	1.0706	2.0	1.1063	3.0	1.1420	4.0	1.1778
0.25	1.0	0.5773	2.0	0.5976	3.0	0.6179	4.0	0.6381
0.50	1.0	0.1593	2.0	0.1682	3.0	0.1772	4.0	0.1861
0.75	1.0	1.2277	2.0	1.2656	3.0	1.3034	4.0	1.3412
1.00	1.0	2.7966	2.0	2.8450	3.0	2.8934	4.0	2.9418

TABLE 11. Influence of Schmidt number on skin friction coefficient.

η	Sc	Cf	Sc	Cf	Sc	Cf	Sc	Cf
0.00	1.0	1.0591	2.0	1.0901	3.0	1.1162	4.0	1.1375
0.25	1.0	0.5692	2.0	0.5816	3.0	0.5901	4.0	0.5951
0.50	1.0	0.1576	2.0	0.1690	3.0	0.1795	4.0	0.1885
0.75	1.0	1.2133	2.0	1.2388	3.0	1.2577	4.0	1.2711
1.00	1.0	2.7764	2.0	2.8040	3.0	2.8232	4.0	2.8360

TABLE 12. Influence of chemical reaction parameter on skin friction coefficient.

η	Kr	Cf	Kr	Cf	Kr	Cf	Kr	Cf
0.00	2.0	1.0266	4.0	1.0060	6.0	0.9894	8.0	0.9757
0.25	2.0	0.5521	4.0	0.5399	6.0	0.5300	8.0	0.5217
0.50	2.0	0.1485	4.0	0.1439	6.0	0.1403	8.0	0.1376
0.75	2.0	1.1808	4.0	1.1583	6.0	1.1398	8.0	1.1243
1.00	2.0	2.7362	4.0	2.7063	6.0	2.6813	8.0	2.6600

From table 19 to 21, it is clear that the heat transfer coefficient Nu decreases at the cold wall and increases at the heated wall on increasing the Prandtl number Pr absorption of radiation parameter Q and chemical reaction parameter Kr.

TABLE 13. Influence of cold wall slip parameter on skin friction coefficient.

η	γ	Cf	γ	Cf	γ	Cf	γ	Cf
0.00	0.0	1.3452	0.1	1.0456	0.2	0.8551	0.3	0.7233
0.25	0.0	0.7154	0.1	0.5631	0.2	0.4662	0.3	0.3992
0.50	0.0	0.0721	0.1	0.1530	0.2	0.2044	0.3	0.2400
0.75	0.0	1.1531	0.1	1.2013	0.2	1.2319	0.3	1.2531
1.00	0.0	2.7264	0.1	2.7628	0.2	2.7859	0.3	2.8019

TABLE 14. Influence of heated wall slip parameter on skin friction coefficient.

η	σ	Cf	σ	Cf	σ	Cf	σ	Cf
0.00	0.0	1.2117	0.1	1.0456	0.2	0.7842	0.3	0.3129
0.25	0.0	0.7344	0.1	0.5631	0.2	0.2936	0.3	0.1925
0.50	0.0	0.0710	0.1	0.1530	0.2	0.5054	0.3	1.1408
0.75	0.0	0.8727	0.1	1.2013	0.2	1.7182	0.3	2.6502
1.00	0.0	2.2595	0.1	2.7628	0.2	3.5544	0.3	4.9821

TABLE 15. Influence of radiation parameter on heat transfer coefficient.

η	N	Nu	N	Nu	N	Nu	N	Nu
0.00	1.0	-1.1356	2.0	-1.0892	3.0	-1.0664	4.0	-1.0529
0.25	1.0	-1.0637	2.0	-1.0430	3.0	-1.0325	4.0	-1.0261
0.50	1.0	-0.9964	2.0	-0.9984	3.0	-0.9991	4.0	-0.9995
0.75	1.0	-0.9346	2.0	-0.9562	3.0	-0.9671	4.0	-0.9737
1.00	1.0	-0.8784	2.0	-0.9169	3.0	-0.9369	4.0	-0.9491

TABLE 16. Influence of heat source parameter on heat transfer coefficient.

η	H	Nu	H	Nu	H	Nu	H	Nu
0.00	1.0	-1.1735	2.0	-1.0672	3.0	-0.9734	4.0	-0.8903
0.25	1.0	-1.0620	2.0	-0.9868	3.0	-0.9196	4.0	-0.8592
0.50	1.0	-0.9818	2.0	-0.9650	3.0	-0.9480	4.0	-0.9310
0.75	1.0	-0.9288	2.0	-0.9952	3.0	-1.0535	4.0	-1.1047
1.00	1.0	-0.8998	2.0	-1.0748	3.0	-1.2386	4.0	-1.3929

From table 22, it is clear that the mass transfer coefficient Sh decreases at the cold wall and increases at the heated wall on increasing the Schmidt number Sc.

TABLE 17. Influence of Dufour number on heat transfer coefficient.

η	Du	Nu	Du	Nu	Du	Nu	Du	Nu
0.00	1.0	-1.1323	2.0	-0.9662	3.0	-0.8000	4.0	-0.6338
0.25	1.0	-1.0708	2.0	-1.0171	3.0	-0.9635	4.0	-0.9098
0.50	1.0	-1.0016	2.0	-1.0208	3.0	-1.0400	4.0	-1.0593
0.75	1.0	-0.9302	2.0	-0.9939	3.0	-1.0575	4.0	-1.1211
1.00	1.0	-0.8602	2.0	-0.9479	3.0	-1.0356	4.0	-1.1233

TABLE 18. Influence of Schmidt number on heat transfer coefficient.

η	Sc	Nu	Sc	Nu	Sc	Nu	Sc	Nu
0.00	1.0	-1.1864	2.0	-1.0623	3.0	-0.9284	4.0	-0.7892
0.25	1.0	-1.0928	2.0	-1.0776	3.0	-1.0762	4.0	-1.0857
0.50	1.0	-0.9971	2.0	-1.0192	3.0	-1.0433	4.0	-1.0652
0.75	1.0	-0.9061	2.0	-0.9349	3.0	-0.9541	4.0	-0.9655
1.00	1.0	-0.8234	2.0	-0.8475	3.0	-0.8571	4.0	-0.8594

TABLE 19. Influence of Prandtl number on heat transfer coefficient.

η	Pr	Nu	Pr	Nu	Pr	Nu	Pr	Nu
0.00	0.71	-1.2320	1.00	-1.3352	5.00	-3.0572	7.00	-4.0049
0.25	0.71	-1.1030	1.00	-1.1403	5.00	-1.3193	7.00	-1.2407
0.50	0.71	-0.9901	1.00	-0.9806	5.00	-0.7169	7.00	-0.6036
0.75	0.71	-0.8861	1.00	-0.8499	5.00	-0.4801	7.00	-0.4161
1.00	0.71	-0.8075	1.00	-0.7429	5.00	-0.3638	7.00	-0.3275

TABLE 20. Influence of absorption of radiation parameter on heat transfer coefficient.

η	Q	Nu	Q	Nu	Q	Nu	Q	Nu
0.00	1.0	-1.3171	2.0	-1.4386	3.0	-1.5602	4.0	-1.6817
0.25	1.0	-1.1622	2.0	-1.2468	3.0	-1.3314	4.0	-1.4159
0.50	1.0	-1.0014	2.0	-1.0176	3.0	-1.0338	4.0	-1.0500
0.75	1.0	-0.8387	2.0	-0.7626	3.0	-0.6864	4.0	-0.6103
1.00	1.0	-0.6761	2.0	-0.4884	3.0	-0.3006	4.0	-0.1128

From table 23, it is clear that the mass transfer coefficient Sh increases at the cold wall and decreases at the heated wall on increasing the chemical reaction parameter Kr.

TABLE 21. Influence of chemical reaction parameter on heat transfer coefficient.

η	Kr	Nu	Kr	Nu	Kr	Nu	Kr	Nu
0.00	2.0	-1.2722	4.0	-1.3153	6.0	-1.3494	8.0	-1.3769
0.25	2.0	-1.1276	4.0	-1.1547	6.0	-1.1769	8.0	-1.1953
0.50	2.0	-0.9935	4.0	-0.9987	6.0	-1.0045	8.0	-1.0105
0.75	2.0	-0.8693	4.0	-0.8452	6.0	-0.8264	8.0	-0.8116
1.00	2.0	-0.7529	4.0	-0.6872	6.0	-0.6279	8.0	-0.5737

TABLE 22. Influence of Schmidt number on mass transfer coefficient.

η	Sc	Sh	Sc	Sh	Sc	Sh	Sc	Sh
0.00	1.0	-1.4593	2.0	-1.9866	3.0	-2.5563	4.0	-3.1488
0.25	1.0	-1.1559	2.0	-1.2500	3.0	-1.2820	4.0	-1.2635
0.50	1.0	-0.9517	2.0	-0.8650	3.0	-0.7652	4.0	-0.6709
0.75	1.0	-0.8190	2.0	-0.6742	3.0	-0.5720	4.0	-0.5064
1.00	1.0	-0.7383	2.0	-0.5919	3.0	-0.5187	4.0	-0.4863

TABLE 23. Influence of chemical reaction parameter on mass transfer coefficient.

η	Kr	Sh	Kr	Sh	Kr	Sh	Kr	Sh
0.00	2.0	-1.0981	4.0	-0.9184	6.0	-0.7762	8.0	-0.6620
0.25	2.0	-0.9826	4.0	-0.8536	6.0	-0.7487	8.0	-0.6620
0.50	2.0	-0.9521	4.0	-0.9183	6.0	-0.8844	8.0	-0.8510
0.75	2.0	-0.9926	4.0	-1.1034	6.0	-1.1894	8.0	-1.2568
1.00	2.0	-1.0970	4.0	-1.4184	6.0	-1.7052	8.0	-1.9651

5. CONCLUSION

In this paper we have studied analytically, Dufour and heat source effects on radiative MHD slip flow of a viscous fluid in a parallel porous plate channel in presence of chemical reaction.Conclusions more important of the study are as follows:

- Thermal Grashof number, Solutal Grashof number, pressure gradient, Darcy parameter, Prandtl number, absorption of radiation parameter and Schmidt number are tend to accelerate the fluid velocity and skin friction coefficient at both cold and heated plates.
- Magnetic parameter, radiation parameter, heat source parameter, Dufour number and chemical reaction parameter are tend to decelerate the fluid velocity and skin friction coefficient at both cold and heated plates.
- On increasing the slip parameter at the cold wall the velocity increases whereas the effect is totally reversed in the case of shear stress at the cold wall.

- Temperature profiles are increases on increasing the Prandtl number, absorption of radiation parameter and chemical reaction parameter whereas the effect is totally reversed in the case of heat transfer coefficient at the cold wall.
- Temperature profiles are decreases on increasing the heat source parameter, radiation parameter, Dufour number and Schmidt number whereas the effect is totally reversed in the case of heat transfer coefficient at the cold wall.
- Concentration profiles are increases on increasing the Schmidt number whereas the effect is totally reversed in the case of mass transfer coefficient at the cold wall.
- Concentration profiles are decreases on increasing the chemical reaction parameter whereas the effect is totally reversed in the case of mass transfer coefficient at the cold wall.

ACKNOWLEDGEMENTS

Authors are thankful for the suggestions and comments of the referees, which have led to improvement of the paper.

REFERENCES

[1] C. L. M. H. Navier: *Memoire Surles du Movement des*, Mem Acad. Sci. Inst. France, **1**(1823), pp. 414-416.

[2] M. J. Martin and I.D. Boyd: *Blasius boundary layer solution with slip flow conditions, Rarefied Gas Dynamics*: 22nd International Symposium, Sydney, Australia, July 9–14, T. J. Bartel and M. A. Gallis, eds., American Institute of Physics, AIP Conf. Proc., **585**(2001), pp. 518–523.

[3] H. I. Anderson: *Slip Flow Past a Stretching Surface*, Acta Mech., **158**(2002), pp. 121–125.

[4] T. Fang and C. F. Lee: *A moving-wall boundary layer flow of a slightly rarefied gas free stream over a moving flat plate*, Appl. Math. Lett., **18**(2005), pp. 487–495.

[5] Yu S and Ameel T. A: *Slip-flow heat transfer in rectangular microchannels*, Int. J. Heat Mass Transfer, 44 (2002) pp. 4225-4234.

[6] F. Soltani and U. Yilmazer: *Slip velocity and slip layer thickness in flow of concentrated suspensions*, J. Appl. Polym. Sci, **70** (1998), pp. 515-522.

[7] N. K. Vedantam and R. N. Parthasarathy: *Effects of slip on the flow characteristics of laminar flat plate boundary-layer*, Proceedings of ASME Fluids Engineering Summer Meeting, Miami, FL, 2006, pp. 1551–1560.

[8] M.J. Martin and I. D. Boyd: *Momentum and heat transfer in a laminar boundary layer with slip flow*, J. Thermophys. Heat Transfer, **20**(2006), pp. 710–719.

[9] M, Venkateswarlu and P. Padma: *Unsteady MHD free convective heat and mass transfer in a boundary layer flow past a vertical permeable plate with thermal radiation and chemical reaction*, Procedia Engineering , **127**(2015), pp. 791-799.

[10] K. Watanebe , Yanuar and H. Mizunuma: *Slip of Newtonian fluids at solid boundary*, JSME Int. J. Ser. B, **41**(1998), pp. 525-529.

[11] E. Ruckenstein and P. Rajora: *On the no-slip boundary conditions of hydrodynamics*, J. Colloid Interface Sci, **96** (1983), pp. 488-491.

[12] K. Cao and J. Baker*: Slip Effects on mixed convective flow and heat transfer from a vertical plate*, Int. J. Heat Mass Transfer, 52(2009), pp. 3829–3841.

[13] A. Aziz: *Hydrodynamic and thermal slip flow boundary layers over a flat plate with constant heat flux boundary condition*, Commun. Nonlinear Sci. Numer. Simul., **15**(2010), pp. 573–580.

[14] M. Venkateswarlu and D. Venkata Lakshmi*: Slip velocity distribution on MHD oscillatory heat and mass transfer flow of a viscous fluid in a parallel plate channel*, GANIT J.Bangladesh Math. Soc, **36**(2016), pp. 93-114.

[15] K. Bhattacharyya, Mukhopadhyay and G. C. Layek: *MHD boundary layer slip flow and heat transfer over a flat plate*, Chinese Phys. Lett., 28(2011), p. 024701.

[16] M. J. Martin and I. D. Boyd: *Falkner-Skan flow over a wedge with slip boundary conditions*, J. Thermophys. Heat transfer, **24**(2010), pp. 263–270.

[17] M.M. Rahman and I. A. Eltayeb: *Convective slip flow of rarefied fluids over a wedge with thermal jump and variable transport properties*, Int. J. Therm. Sci., **50**(2011), pp. 468–479.

[18] Jr. W. Marques, G. M. Kremer and F. M. Shapiro: *Coutte flow with slip and jump boundary conditions*, Continumm Mech. Thermodynam, **12** (2000), pp.379-386.

[19] M, Turkyilmazoglu: *Multiple analytic solutions of heat and mass transfer of magnetohydrodynamic slip flow for two types of viscoelastic fluids over a stretching surface*, ASME J. Heat Transfer, **134**(2012), p. 071701.

[20] U. N. Das, R. K. Deka, V. M. Soundalgekar: *Effect of mass transfer on flow past an impulsively started infinite vertical plate with constant heat flux and chemical reaction*, Forschung Ingenieurwesen-Engineering research Bd, **60**(1994), pp.:284–287.

[21] J. Manjula , P. Padma , M. Gnaneswara Reddy and M. Venakateswarlu : *Influence of thermal radiation and chemical reaction on MHD flow, heat and mass transfer over a stretching surface*, Procedia Engineering, **127** (2015), pp. 1315-1322.

[22] R. Muthucumarswamy, P. Ganesan: *Diffusion and first-order chemical reaction on impulsively started infinite vertical plate with variable temperature*, Int. J . Therm Sci, **41**(2002), pp.475–479.

[23] K. V. Prasad, S. Abel and P. S. Datti: *Diffusion of chemically reactive species of a non-Newtonian fluid immersed in a porous medium over a stretching sheet*, Int. J. Non-Linear Mech, **38**(2003), pp. 651–657.

[24] M. Venkateswarlu , G. V. Ramana Reddy and D. V. Lakshmi: *Diffusion-thermo effects on MHD flow past an infinite vertical porous plate in the presence of radiation and chemical reaction*, International Journal of Mathematical Archive, **4**(2013), pp. 39-51.

[25] M. Venkateswarlu, G. V. Ramana Reddy and D. V. Lakshmi: *Effects of chemical reaction and heat generation on MHD boundary layer flow of a moving vertical plate with suction and dissipation*, Engineering International, **1**(2013), pp.27-38, 2013.

[26] F. T. Akyildiz, H. Bellout and K. Vajravelu:*Diffusion of chemically reactive species in a porous medium over a stretching sheet*, J. Math Anal Appl., **320**(2006), pp. 322–339.

[27] A. Y. Ghaly and M. A. Seddeek: *Chebyshev finite difference method for the effect of chemical reaction, heat and mass transfer on laminar flow along a semiinfinite horizontal plate with temperature dependent viscosity*, Choas Solitons Fractals ,**19**(2004), pp. 61–70.

[28] E. M. Sparrow and R. D. Cess: *Temperature dependent heat sources or sinks in a stagnation point flow*, Appl. Sci. Res., **10**(1961), pp. 185-197.

[29] M. Venkateswarlu, D. Venkata Lakshmi and K. Nagamalleswara Rao: *Soret, hall current, rotation, chemical reaction and thermal radiation effects on unsteady MHD heat and mass transfer natural convection flow past an accelerated vertical plate*, J. Korean Soc. Ind. Appl. Math., **20**(2016), pp. 203 -224.

[30] M. Venkateswarlu, G. V. Ramana Reddy and D. V. Lakshmi: *Radiation effects on MHD boundary layer flow of liquid metal over a porous stretching surface in porous medium with heat generation*, J. Korean Soc. Ind. Appl. Math., **19**(2015), pp.83- 102.

[31] M. Venkateswarlu, G. V. Ramana Reddy and D. V. Lakshmi: *Thermal diffusion and radiation effects on unsteady MHD free convection heat and mass transfer flow past a linearly accelerated vertical porous plate with variable temperature and mass diffusion*, J. Korean Soc. Ind. Appl. Math., **18**(2014), pp. 257-268.

[32] A. Ishak: *Mixed convection boundary layer flow over a horizontal plate with thermal radiation*, Heat and Mass Transfer, **46** (2009), pp.147–151.

[33] M. Venkateswarlu, D. Venkata Lakshmi and G. Darmaiah: *Influence of slip condition on radiative MHD flow of a viscous fluid in a parallel porous plate channel in presence of heat absorption and chemical reaction* , J. Korean Soc. Ind. Appl. Math., **20**(2016), pp. 333 -354.

[34] E. Magyari and A. Pantokratoras: *Note on the effect of thermal radiation in the linearized Rosseland approximation on the heat transfer characteristics of various boundary layer flows*, Int. Commun. Heat and Mass Transfer, **38**(2011), pp. 554–556.

[35] M. Venkateswarlu, G. Venkata Ramana Reddy and D. Venkata Lakshmi: *Radiation and chemical reaction effects on MHD flow past an oscillating vertical porous plate with constant heat flux*, Proceedings of International Conference on Mathematical Sciences, ISBN-978-93-5107-261-4, 2014, pp.323-327.

[36] S. O. Adesanya and O. D.... Makinde: *MHD oscillatory slip flow and heat transfer in a channel filled with porous media*, U.P.B. Sci. Bull., Series A, **76**(2014), pp.197-204.

[37] N. Siva Kumar, Rushi Kumar and A. G. Vijaya Kumar: *Thermal diffusion and chemical reaction effects on unsteady flow past a vertical porous plate with heat source dependent in slip flow regime*, Journal of Naval Architecture and Marine Engineering, **13**(2016), pp. 51-62.

[38] M. Venkateswarlu and D. Venkata Lakshmi: *Soret and chemical reaction effects on the radiative MHD flow from an infinite vertical plate*, J. Korean Soc. Ind. Appl. Math., **21**(2017), pp. 39 - 61.